

Metallophilic Interactions in Closed-Shell Copper(I) Compounds— A Theoretical Study

Holger L. Hermann,^[a] Gernot Boche,^[b] and Peter Schwerdtfeger*^[a]

Abstract: Cuprophilic interactions in neutral perpendicular model dimers of the type $(\text{CH}_3\text{CuX})_2$ ($\text{X} = \text{OH}_2, \text{NH}_3, \text{SH}_2, \text{PH}_3, \text{N}_2, \text{CO}, \text{CS}, \text{CNH}, \text{CNLi}$) were analyzed by ab initio quantum-chemical methods. The basis set superposition error for the weakly interacting CH_3CuX subunits is significant and is discussed in detail. A new correlation-consistent pseudopotential valence basis set for Cu, derived at the second-order Møller–Plesset level suppresses considerably the basis set superposition error in Cu–Cu interactions compared to the standard Hartree–Fock optimized va-

lence basis set. This allowed the first accurate predictions of cuprophilicity, which has been the subject of considerable debate in the past. The dependence of the strength of cuprophilic interactions on the nature of the ligand X was addressed. The Cu–Cu interaction increases with increasing σ -donor and π -acceptor capability of the ligand and is approximately one-third of the well-

documented aurophilic interactions. By fitting our potential-energy data to the Hershbach–Laurie equation, we determined a relation between the Cu–Cu bond length and the Cu–Cu force constant; this is important for future studies on vibrational behaviour. The role of relativistic effects on the structure and the interaction energy is also discussed. Finally we investigated cuprophilic interactions in $(\text{CH}_3\text{Cu})_4$ as a model species for compounds isolated and characterized by X-ray diffraction.

Keywords: ab initio calculations • closed-shell interactions • copper • metal–metal interactions

Introduction

Complexes of Group 11 metals in the +I oxidation state have a well-known tendency to form clusters, often with quite short metal–metal bond lengths.^[1] Such closed-shell interactions (CSI) often result in unusual chemical and physical properties.^[2] Almost two decades ago, several crystallographic, spectroscopic, and theoretical studies yielded the first evidence for CSIs in Group 11 compounds, often termed $d^{10}–d^{10}$ interactions.^[3–5] The CSIs can range from extremely weak dispersive-type interactions, as in He_2 (dissociation energy $E_d = 2 \times 10^{-2} \text{ kcal mol}^{-1}$), to large charge-induced dipole interactions, as in in the $s^2–s^2$ system AuBa^- ($E_d = 34 \text{ kcal mol}^{-1}$).^[6] Strong closed-shell interactions in inorganic compounds were recently reviewed by Pyykkö.^[7]

The unusually strong CSIs between gold atoms in Au^I compounds initiated a large number of experimental^[8] and

theoretical investigations.^[9–11] Although CSIs are not comparable in strength to normal covalent or ionic bonds, in Au^I compounds they can be as large as $7–12 \text{ kcal mol}^{-1}$, which is within the range of typical hydrogen bonds. The interplay between correlation and relativistic effects is mainly responsible for these aurophilic attractions,^[9, 10] although ionic contributions cannot completely be neglected.^[11] Such aurophilic interactions are also thought to be responsible for the luminescent behavior of a number of gold compounds.^[12]

Here we draw attention to $\text{Cu}^I–\text{Cu}^I$ CSIs, which have been proposed but studied only little in the past.^[10, 13–16] In the case of Cu^I , early extended Hückel (EHT) calculations support hybridization effects between filled $(n-1)d$ orbitals and the ns and np orbitals.^[17] For example, Hollander and Coucouvanis^[18] found little sensitivity of the copper–copper distance to the nature of the ligands in a number of octameric copper compounds and, hence, predicted the presence of Cu–Cu interactions. However, others dispute the existence of such interactions^[19] and prefer the terminology of nonbonding close $\text{Cu}^I–\text{Cu}^I$ contacts.^[20] Previous theoretical studies on cuprophilic interactions were plagued with rather large basis set superposition errors due to the limited basis sets used.^[10, 13, 21]

The debate on cuprophilic interactions is perhaps similar to the discussion a decade ago on the existence of $\text{Tl}^I–\text{Tl}^I$

[a] Prof. Dr. P. Schwerdtfeger, Dr. H. L. Hermann
Department of Chemistry, The University of Auckland
Private Bag 92019, Auckland (New Zealand)
Fax: (+64)9-3737422
E-mail: schwerd@ccu1.auckland.ac.nz

[b] Prof. Dr. G. Boche
Philipps-Universität Marburg
Fachbereich Chemie
35032 Marburg (Germany)

interactions in the solid state, postulated by Schumann et al.^[22] and later supported by EHT calculations by Janiak and Hoffmann, which predicted large overlap effects between TI atoms.^[23] However, s^2-s^2 CSIs in TI^I compounds proved to be extremely weak when more accurate ab initio methods were applied.^[24]

Nevertheless, there is mounting evidence for $\text{Cu}^I\text{-Cu}^I$ interactions from the short metal-metal distances (usually between 260 and 350 pm)^[25] in several crystal structures. For example, copper-containing organometallic compounds of the type Cu_nR_n ($n = 3-5$),^[26] as shown in Figure 1,^[27-29] have been the subject of discussion ever since their discovery.

However, it is questionable whether the short Cu-Cu contacts in these compounds are due to the constraints of the ring or to metal-metal interactions. This is similar to the ongoing discussion on cuprite (Cu_2O), which was studied in the past^[21] and was recently the subject of intense controversy.^[30]

Further evidence for cuprophilic interactions was recently found by Boche et al., who crystallized cuprates such as $[\text{tBuCu}(\text{CN})\text{Li}(\text{Et}_2\text{O})_2]_\infty$ (**4**),^[31] and $[[[(\text{Me}_3\text{Si})\text{CH}_2]_2\text{CuLi}]_2(\text{Et}_2\text{O})_3]$ (**5**),^[32] (Figure 2). In both compounds the monomeric cuprate units are nearly orthogonal to each other ($\delta(\text{C-Cu-Cu-C}) = 94.9^\circ$ in **4**, $\delta(\text{C-Cu-Cu-C}) = 93.7^\circ$ in **5**), and this allows Cu-Cu interaction without steric repulsion of the ligands. Compound **4** has a relatively short Cu-Cu distance of $r(\text{Cu-Cu}) = 271.3$ pm and a mean C-Cu-C bond angle of $\alpha(\text{C-Cu-C}) = 170.0^\circ$, while **5** has $r(\text{Cu-Cu}) = 283.8$ pm and $\alpha(\text{C-Cu-C}) = 172.1^\circ$. In contrast to other structures in which the Cu atoms are brought into close proximity by ligand complexation, in **4** there is no obvious reason why the monomeric units should bend towards each other. The authors furthermore concluded that lithium cuprate dimers of the lithium contact ion pair type, which are formed especially in solvents that poorly solvate lithium ions,^[33] are the reactive species in the addition of cuprates to enones. Further structural and Raman spectroscopic evidence for cuprophilicity was found recently by Che et al. in a lumines-

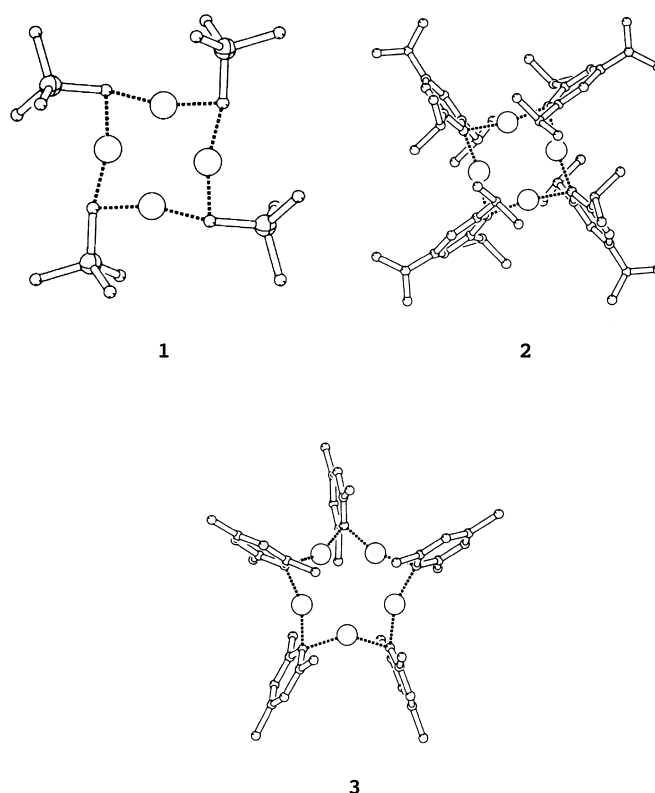


Figure 1. X-ray crystal structures of organocopper compounds of the type $[\text{Cu}_n\text{R}_n]$ ($n = 4, 5$). Selected structural data for $[\text{Cu}_4(\text{CH}_2\text{SiMe}_3)_4]$ ^[27] (**1**): $r(\text{Cu-Cu}) = 241.8$ pm, $r(\text{Cu-C}) = 198.0-204.0$ pm, $\alpha(\text{Cu-C-Cu}) = 73.4/73.8^\circ$, $\alpha(\text{C-Cu-C}) = 163.4/163.7^\circ$; for $[\text{Cu}_4(2,4,6\text{-iPr}_3\text{C}_6\text{H}_2)_4]$ ^[28] (**2**): $r(\text{Cu-Cu}) = 244.5$ pm, $r(\text{Cu-C}) = 195.8-201.8$ pm, $\alpha(\text{C-Cu-C}) = 169.8^\circ$; and for $[\text{Cu}_5(2,4,6\text{-Me}_3\text{C}_6\text{H}_2)_5]$ ^[29] (**3**): $r(\text{Cu-Cu}) = 244.0-255.0$ pm, $r(\text{Cu-C}) = 191.0-202.0$ pm, $\alpha(\text{Cu-C-Cu}) = 78.0-80.0^\circ$, $\alpha(\text{C-Cu-C}) = 149.0-160.0^\circ$.

cent binuclear copper(I) complex.^[34] For $[\text{Cu}_2(\text{dcpm})_2]\text{X}_2$ ($\text{X} = \text{ClO}_4^-$, $\text{dcpm} = \text{bis}(\text{dicyclohexylphosphanyl})\text{methane}$) with $r(\text{Cu-Cu}) = 273.1$ pm, Che et al. could assign the Raman

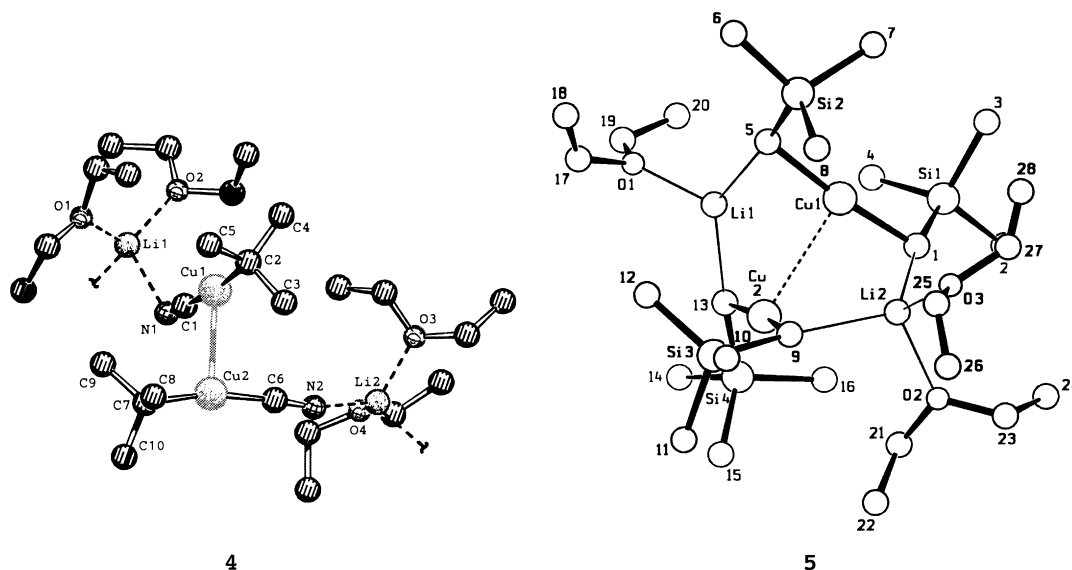


Figure 2. Solid-state structures of $[[\text{tBuCu}(\text{CN})\text{Li}(\text{Et}_2\text{O})_2]_\infty]$ ^[31] (**4**) and $[[[(\text{Me}_3\text{Si})\text{CH}_2]_2\text{CuLi}]_2(\text{Et}_2\text{O})_3]$ ^[32] (**5**). Selected bond lengths [pm], angles $^\circ$, and dihedral angles $^\circ$ in **4**: C1-Cu1 187.8, C2-Cu1 196.9, Cu1-Cu2 271.3, C1-Cu1-C2 170.0, C2-Cu1-Cu2 103.4, C1-Cu1-Cu2-C6 84.6; and in **5**: Cu1-Cu2 283.8, C1-Cu1-C5 172.9, C9-Cu2-C13 171.3, C1-Cu1-Cu2-C9 93.7.

intensity to a single low-frequency mode, namely, that of the Cu¹–Cu¹ stretch ($\nu(\text{Cu}_2) = 104 \text{ cm}^{-1}$).

To investigate CSIs in Cu–Cu contacts we performed ab initio calculations on a wide variety of monomeric (CH_3CuX) (**6**) and dimeric Cu¹ compounds ($(\text{CH}_3\text{CuX})_2$ (**7**; $\text{X} = \text{OH}_2$, NH_3 , SH_2 , PH_3 , N_2 , CO , CS , CNH , CNLi) to model the solid state. We also investigated the Cu–Cu interactions in the CH_3 -bridged tetramer $(\text{CH}_3\text{Cu})_4$ (**8**) as a model compound for **1** or **2**.

Computational Methods

All calculations were performed with the Gaussian 98^[35] program package. The heteroatoms of all model compounds were treated with all-electron standard basis sets,^[36] while for copper either an energy-consistent scalar relativistic or a nonrelativistic (NR) 19 valence electron (19-VE) small-core pseudopotential (PP) of the Stuttgart group^[37] was used to replace the inner core electrons.

Three different basis sets were applied to describe the copper valence electron region (see Table 1). The originally published Hartree–Fock (HF) optimized Cu basis set of the Stuttgart group^[37] is denoted as basis 1a, basis 1b is derived from 1a but augmented by two f-type polarization functions,^[10] and basis 2 is a large correlation-consistent Gaussian-type basis set generated in our group (Table 2).

Basis 2a was obtained by numerically optimizing a (9s8p6d4f) subset of exponents for the Cu atom at the second-order Møller–Plesset level (MP2). Furthermore, a (2s1p1d) set of diffuse functions was added which we obtained from a numerical fit procedure at the MP2 level for the Cu[−] anion to reproduce the experimentally known value for the electron affinity E_A of Cu at the coupled cluster [CCSD(T)] level of theory. The calculated CCSD(T) ionization potential of 7.71 eV and electron affinity of 1.18 eV are in excellent agreement with the experimental values of 7.72 and 1.23 eV.^[38] Correlation-consistent basis sets optimized by this procedure

Table 1. Basis sets^[a] and calculated total electronic energies E [au] for the Cu atoms used in the present work.

Case	Atom	Basis	$E(\text{HF})$	$E(\text{MP2})$	$E(\text{CCSD(T)})$
1a	H,Li,C,N,O,P,S	6-31 + G(d)	–	–	–
	Cu	(8s6p5d)/[6s5p3d]	−196.16955	−196.54767	−196.49965
1b	Cu ^[b]	(8s6p5d2f)/[6s5p3d2f]	−196.16955	−196.73788	−196.69156
2a	H	cc-pVDZ	–	–	–
	C,N ^[c] ,O,P,S	cc-PVTZ	–	–	–
	Li	6-31 + (d,p)	–	–	–
	Cu ^[d]	(11s9p7d4f)/[9s7p5d3f]	−196.20483	−197.10982	−197.02541
			(−196.20500)	(−197.13703)	(−197.05210)
2b	Cu NR ^[e]	(11s9p7d4f)/[9s7p5d3f]	−195.61745	−196.51414	−196.43161

[a] Cu valence basis sets for the Stuttgart small-core pseudopotentials (PP) of the Stuttgart group.^[37] [b] The f exponents are $\alpha_f = 0.24, 3.70$.^[10] [c] In the case of $\text{X} = \text{CNH}$ and CNLi the cc-pVDZ basis set was used for N. [d] Energy values E in parentheses are for the uncontracted basis set. [e] NR indicates that a nonrelativistic PP was used instead.^[37]

Table 2. Exponents and coefficients for the correlation-consistent Cu valence basis set.^[a]

exp.	s		p		d		f	
	coeff.	exp.	coeff.	exp.	coeff.	exp.	coeff.	
27.53091	−0.10565	79.14552	0.00247	50.18287	0.02203	11.60973	0.11427	
14.59263	0.29217	17.22254	−0.07389	15.66677	0.10969	4.67063	0.33370	
6.15443	0.62754	7.69319	0.02583	5.69954	0.25889	1.85482	–	
4.89927	–	4.00736	–	2.13198	–	0.58635	–	
2.36351	–	1.86406	–	0.74071	–	–	–	
1.13720	–	0.85030	–	0.21651	–	–	–	
0.50889	–	0.36183	–	0.05492	–	–	–	
0.26090	–	0.12873	–	–	–	–	–	
0.12573	–	0.04036	–	–	–	–	–	
0.06667	–	–	–	–	–	–	–	
0.02409	–	–	–	–	–	–	–	

[a] The basis set was numerically optimized at the scalar relativistic MP2 level of theory.

have been repeatedly used^[39] to successfully suppress what is known as the basis set superposition error (BSSE).^[40] Basis 2b is in principle of the same size as basis 2a, except that a nonrelativistic (NR) pseudopotential^[37] was used for copper.

The structures of all monomeric compounds of type CH_3CuX (**6**; $\text{X} = \text{OH}_2$, NH_3 , SH_2 , PH_3 , N_2 , CO , CS , CNH , CNLi) were fully optimized at the pseudopotential (PP) MP2 level (Table 3), while keeping the orbital space fully active.^[41] The geometries were proven to be minima by analyzing the second derivative matrix (Hessian), at least for basis sets 1a and 1b. The unchanged monomer geometries were used to build up the perpendicular (C_2 -symmetric) dimers $(\text{CH}_3\text{CuX})_2$ (**7**; Figure 3).

The Cu¹–Cu¹ attraction in those dimers was then studied by varying the Cu–Cu distance $r(\text{Cu}-\text{Cu})$. The attraction energies of the two interacting closed-shell fragments were obtained with (ΔE_{CP}) and without (ΔE) counterpoise (CP) corrections according to Equations (1) and (2). If not otherwise stated, CP corrections to eliminate the BSSE were performed for the monomers at the equilibrium distances of the dimers.

$$\Delta E = E_{\text{AB}}^{(\text{AB})} - E_{\text{A}}^{(\text{A})} - E_{\text{B}}^{(\text{B})} \quad (1)$$

$$\Delta E_{\text{CP}} = E_{\text{AB}}^{(\text{AB})} - E_{\text{A}}^{(\text{AB})} - E_{\text{B}}^{(\text{AB})} \quad (2)$$

For the dimers **7** the Cu–Cu distance was varied to produce potential energy curves and subsequently fitted to a Morse potential [Eq. (3)] to correctly describe the dissociation limit into two closed-shell monomer fragments CH_3CuX **6**. This gives both accurate Cu–Cu bond lengths and force constants in agreement with values obtained by the more accurate analytical optimization techniques used for the smaller basis sets.

$$V(r_{\text{Cu}-\text{Cu}}) = D(1 - \exp^{-a(r-r_{\text{eq}})})^2 \quad (3a)$$

$$k_{\text{Cu}-\text{Cu}} = 2Da^2 \quad (3b)$$

For the geometry optimization of $(\text{CH}_3\text{Cu})_4$ (**8**) we used the less computer extensive Los Alamos basis sets and pseudopotentials (LANL2DZ).^[35]

The natural bond orbital (NBO) analysis of Reed and Weinhold^[42] within the Gaussian 98 program suite^[35] was used to determine natural atomic charges and bonding contributions.

Results and Discussion

Monomers: Table 3 lists the geometric parameters for the monomers H_3CCuX (**6**; $\text{X} = \text{OH}_2$, NH_3 , SH_2 , PH_3 , N_2 , CO , CS , CNH , CNLi) together with the bond dissociation energies for the reaction $\text{H}_3\text{CCuX} \rightarrow \text{CH}_3\text{Cu} + \text{X}$ with (ΔE_{ZPVE}) and without (ΔE) correction for the zero-point vibrational energy. All the monomers were fully optimized at the MP2 level by using the basis sets and pseudopotentials listed in Table 1.

The monomers **6** are in general linear (see Figure 3) with $\alpha(\text{C}-\text{Cu}-\text{X}) = 180^\circ$, except for $\text{X} = \text{OH}_2$ and SH_2 , for which they are slightly bent ($\alpha(\text{C}-\text{Cu}-\text{O}) = 179.2^\circ$ and $\alpha(\text{C}-\text{Cu}-\text{S}) = 178.1^\circ$).

The C–Cu bond length of **6** is sensitive to the nature of X (Figure 4), and $r(\text{C}-\text{Cu})$ varies between

Table 3. Optimized parameters for the H_3CCuX monomers at the MP2 level of theory.^[a]

X	Basis	$r(C-Cu)$	$r(Cu-X)$	$r(X-Y)^{[b]}$	$\alpha(H-C-Cu)$	$\alpha(Cu-X-Y)$	ΔE	ΔE_{ZPVE}
– ^[c]	1a	186.8	–	–	108.8	–	–	–
	1b	184.8	–	–	108.8	–	–	–
	2a	182.4	–	–	108.8	–	–	–
	2b	185.0	–	–	108.9	–	–	–
OH ₂	1a	186.4	195.3	97.7	110.6	112.7	25.5	23.1
	1b	185.3	193.4	97.8	110.2	110.7	28.4	26.0
	2a	183.2	190.8	97.2	111.2	111.4	30.6	–
	2b	184.9	192.5	97.1	111.3	112.1	26.9	–
NH ₃	1a	187.4	193.6	102.2	111.3	111.9	38.3	35.6
	1b	186.5	191.2	102.3	110.9	111.5	42.5	39.8
	2a	184.5	189.4	102.1	110.9	111.5	43.1	–
	2b	186.2	191.0	102.0	111.6	111.9	38.9	–
SH ₂	1a	188.1	219.7	134.5	110.9	102.4	27.2	25.2
	1b	187.0	214.3	134.7	110.8	101.4	34.6	32.6
	2a	185.6	212.1	135.0	111.3	103.2	32.4	–
	2b	187.3	214.8	135.0	111.3	102.7	28.1	–
PH ₃	1a	189.4	216.5	140.7	111.3	118.8	33.5	33.5
	1b	188.3	213.0	140.7	111.0	118.7	40.5	38.4
	2a	186.8	210.0	141.2	111.5	119.4	40.0	–
	2b	188.5	212.4	141.2	111.5	119.4	35.0	–
N ₂	1a	187.6	181.6	113.5	111.0	180.0	19.6	18.0
	1b	187.1	179.4	113.6	110.7	180.0	24.2	22.6
	2a	185.1	176.9	111.7	111.3	180.0	27.6	–
	2b	186.6	179.4	111.5	111.3	180.0	22.7	–
CO	1a	189.2	177.1	115.7	111.3	180.0	34.3	32.4
	1b	188.8	175.8	115.8	110.9	180.0	40.0	38.1
	2a	186.9	172.6	114.3	111.5	180.0	45.1	–
	2b	188.4	175.2	114.1	111.6	180.0	38.6	–
CS	1a	190.1	173.6	154.3	111.4	180.0	51.8	50.1
	1b	189.5	172.7	154.4	111.0	180.0	58.2	56.4
	2a	187.6	169.4	154.4	111.6	180.0	62.2	–
	2b	189.0	171.8	154.1	111.7	180.0	54.6	–
CNH ^[d]	1a	189.4	179.7	118.2	111.6	180.0	41.4	39.8
	1b	188.9	178.1	118.3	111.2	180.0	46.7	45.2
	2a	187.0	175.0	117.4	111.8	180.0	51.7	–
	2b	188.5	177.5	117.2	111.8	180.0	45.7	–
CNLi ^[e]	1a	190.0	182.1	119.2	111.8	180.0	52.0	50.1
	1b	189.2	180.4	119.3	111.5	180.0	57.1	55.2
	2a	187.4	177.7	118.3	112.0	180.0	61.4	–
	2b	188.9	180.1	118.2	112.1	180.0	55.9	–

[a] Bond lengths r in picometers, angles α in degrees. The ΔE values [kcal mol^{-1}] are given for the Cu–X bond strength (dissociation into CuCH_3 and X) with (ΔE_{ZPVE}) and without (ΔE) ZPVE correction. [b] For bond lengths of the unbound ligands X, see ref. [50]. [c] An experimental bond length for CH_3Cu is not available, but there are numerous other ab initio calculations, for example, by Frenking,^[44, 51] Bauschlicher^[43] or Nakamura.^[52] [d] N–H bond lengths for basis sets 1a, 1b, 2a, and 2b are 100.4, 100.4, 100.6, and 100.6 pm, respectively. [e] N–Li bond lengths for basis set 1a, 2b, 2a, and 2b are 179.5, 179.3, 182.1, and 182.4 pm, respectively.

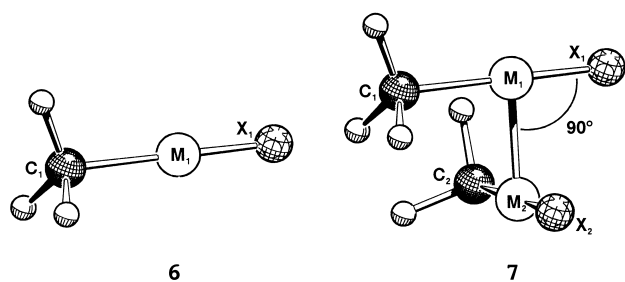


Figure 3. Model monomers **6** and the perpendicular arrangement of two monomers in the dimers **7**. The $C_1-M_1-M_2-C_2$ and $X_1-M_1-M_2-X_2$ dihedral angles are fixed at 90° .

182.3 pm ($X = \text{OH}_2$) and 187.6 pm ($X = \text{CS}$) for basis 2a. One usually expects an elongated C–Cu bond (weaker bonding of CH_3) if the Cu–X bond is strong, but comparing the ΔE values

with the C–Cu bond lengths shows that this is not the case. It is likely that other bonding contributions such as π bonding between the ligand X and Cu are important as well.

The C–Cu and Cu–X bond lengths are sensitive to the basis sets applied, that is, they contract slightly on going from basis 1a to basis 1b and further to the largest basis set 2a. For example, the influence of two additional f functions at Cu (basis 1b vs 1a) on $r(\text{C–Cu})$ is about -1 pm. For $r(\text{Cu–X})$, these changes range from -0.9 ($X = \text{CS}$) to -5.4 pm ($X = \text{SH}_2$). Even more important are the differences between basis sets 1a and 2a. The $r(\text{C–Cu})$ decrease in general by more than 2 pm, while the changes in $r(\text{Cu–X})$ are between -4.2 pm ($X = \text{NH}_3$, CS) and -7.6 pm ($X = \text{SH}_2$). Clearly, variations in the geometry of monomer **6** will influence $\text{Cu}^I\text{–Cu}^I$ interactions in **7**, and it is therefore important to use sufficiently large basis sets.

It has been shown that relativistic effects cannot be neglected in accurate calculations of bond lengths and energies in copper compounds.^[43, 44] The so-called Group 11 maximum of relativistic effects also applies for Cu, although to a lesser extent than for Ag or Au. A comparison of $r(\text{C–Cu})$ and $r(\text{Cu–X})$ calculated with the

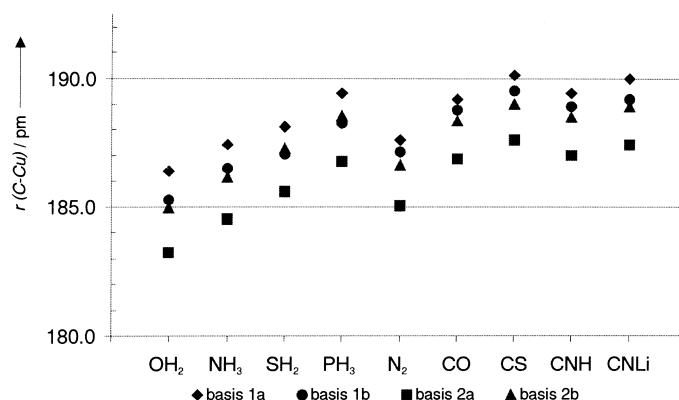


Figure 4. Bond lengths of the monomers **6** calculated (MP2) with basis sets 1a, 1b, 2a, and 2b.

same copper valence basis set but different copper pseudo-potentials, namely, a scalar relativistic (basis 2a) and a non-relativistic (basis 2b) pseudopotential, clearly shows that C–Cu and Cu–X bonds contract by roughly 1.5 and 2.0 pm, respectively, due to relativistic effects. The longer nonrelativistic Cu–X bond lengths correlate to smaller bond dissociation energies ΔE at this level (see Table 3 and Figure 5).

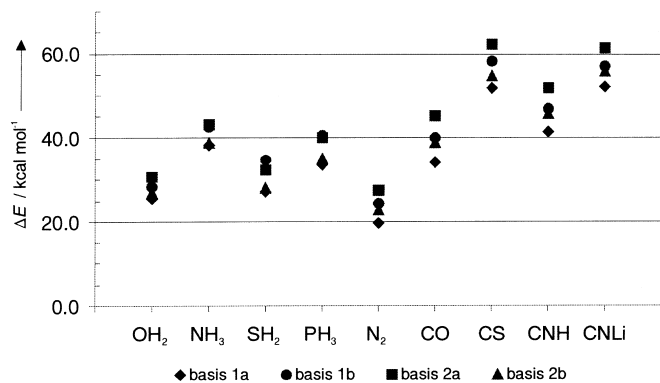


Figure 5. Cu–X bond dissociation energies ΔE of the monomers **6** calculated (MP2) with basis sets 1a, 1b, 2a, and 2b.

Depending on the ligand X, the dissociation energies calculated at the nonrelativistic level are smaller by $3.7 \text{ kcal mol}^{-1}$ (12.1%) for $X = \text{OH}_2$ and $7.6 \text{ kcal mol}^{-1}$ (12.2%) for $X = \text{CS}$ than the values calculated at the relativistic level. This indicates that relativistic effects cannot be neglected for the calculations on the dimeric compounds.

Table 4 summarizes the results of a natural bond orbital analysis (NBO) on the monomers **6**. The copper atoms bear positive charges in the range from $q(\text{Cu}) = +0.44$ ($X = \text{OH}_2$) to $q(\text{Cu}) = +0.76$ ($X = \text{CS}$), while the methyl groups are negatively charged, with values between $q(\text{CH}_3) = -0.53$ ($X = \text{OH}_2$) and $q(\text{CH}_3) = -0.65$ ($X = \text{CNLi}$). The ligands X carry a relatively small positive or negative charge due to their donor or acceptor capabilities. The orbital occupations for the copper $n(4s)$, $n(3d_\sigma)$, $n(3d_\pi)$, and $n(3d_\delta)$ orbitals are also given in Table 4. The copper 4s orbital is populated by $n(4s) = 0.74$ ($X = \text{CS}$) to $n(4s) = 0.83$ ($X = \text{OH}_2$) electrons, while almost no occupation is found for the 4p orbitals ($n(4p) < 0.1$). For all monomers **6** the occupation of the $3d_\delta$ orbitals is essentially 3.92 electrons, while the orbital populations in the 3d orbitals with z contributions ($3d_\sigma$ and $3d_\pi$) vary between 1.70 and 1.95 electrons depending on the ligand X. π -Acceptor ligands (e.g., $X = \text{CO}$, CS) withdraw electron density from the 3d (and 4s) orbitals, as the small $3d_\pi$ populations show, leading to smaller overall occupation numbers of $n(3d) = 9.39$ ($X = \text{CO}$) and $n(3d) = 9.30$ ($X = \text{CS}$) show. In comparison, higher occupation

Table 4. NBO charges for the H_3CCuX (**6**) monomers calculated at the MP2 level with basis set 2a. Cu orbital population for selected valence orbitals.

X	$q(\text{Cu})$	$q(\text{CH}_3)$	$q(\text{X})$	$n(4s)$	$n(3d_\sigma)$	$n(3d_\pi)$	$n(3d_\delta)$
OH_2	0.44	-0.53	0.09	0.83	1.70	3.90	3.92
NH_3	0.45	-0.57	0.12	0.79	1.71	3.90	3.92
SH_2	0.43	-0.58	0.15	0.78	1.79	3.86	3.92
PH_3	0.45	-0.60	0.15	0.76	1.83	3.92	3.91
N_2	0.58	-0.57	-0.01	0.76	1.77	3.76	3.92
CO	0.61	-0.61	0.00	0.78	1.81	3.66	3.91
CS	0.76	-0.62	-0.14	0.74	1.82	3.56	3.91
CNH	0.58	-0.63	0.05	0.77	1.80	3.72	3.92
CNLi	0.52	-0.65	0.13	0.79	1.78	3.78	3.92

numbers between $n(3d) = 9.52$ ($X = \text{OH}_2$) and $n(3d) = 9.57$ ($X = \text{PH}_3$) were determined for the 3d (and 4s) orbitals of σ donors such as $X = \text{OH}_2$, NH_3 , SH_2 , and PH_3 .

Dimers: For the dimers **7** we chose the perpendicular arrangement shown in Figure 3, because such an arrangement minimizes the dipole–dipole interactions between the two subunits **6**, and the undisturbed metal–metal interaction can therefore be studied. These structures are also more closely related to crystal structures, as observed, for example, in the case of **4** and **5**. Therefore, the potential energy curves (Figure 6) do not describe absolute minima on the potential energy surface for the dimeric compounds $(\text{CH}_3\text{CuX})_2$ (**7**), since only the Cu–Cu distances were optimized at fixed monomer geometries.

In Table 5 the calculated data for **7** are summarized. The equilibrium Cu–Cu distances $r_{\text{eq}}(\text{Cu–Cu})$ and the corresponding interaction energies ΔE and ΔE_{CP} are given, as well as the corresponding force constants $k(\text{Cu–Cu})$. In Figure 6 the interaction potentials without counterpoise corrections (basis 2a) are shown.^[45] Note that all interaction potential curves are attractive; this means cuprophilic attraction exists! Furthermore, since all potential energy curves at the HF level are repulsive, cuprophilic interactions can be explained by electron correlation effects.

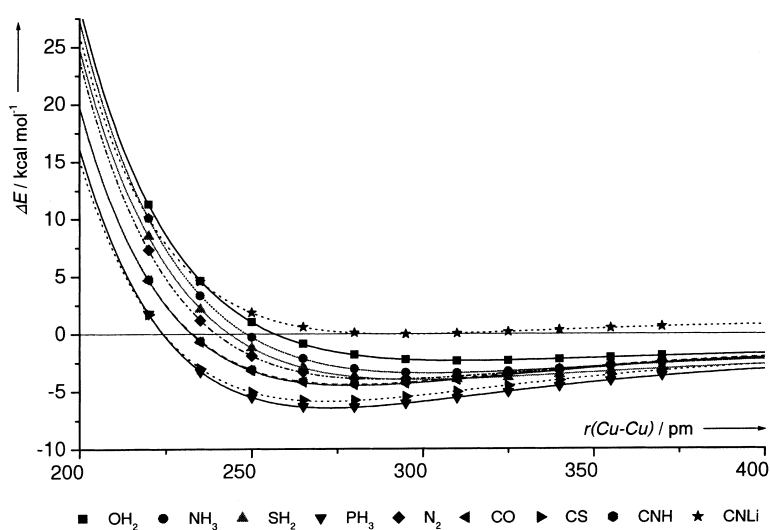


Figure 6. Potential energy curves $\Delta E(r(\text{Cu–Cu}))$ for the dimers **7**. The energy differences ΔE [kcal mol^{-1}] are given relative to the energy of two monomers [Eq. (1)]. Note that these curves do not include counterpoise corrections.

Table 5. Optimized MP2 parameters for the (H₃CCuX)₂ dimers.^[a]

X	Basis	<i>r</i> (Cu–Cu)	<i>k</i> (Cu–Cu)	ΔE	ΔE_{CP}
OH ₂	1a	318.5	–	–2.8	0.2
	1b	287.2	9.45	–4.5	–0.3
	2a	313.9	5.51	–2.4	–1.0
NH ₃	1a	310.2	–	–3.8	–0.3
	1b	283.3	11.32	–5.8	–0.3
	2a	304.3	7.91	–3.4	–1.8
SH ₂	1a	302.9	–	–4.7	0.1
	1b	277.6	12.44	–6.8	0.3
	2a	301.7	8.48	–4.0	–2.2
PH ₃	1a	280.6	–	–6.4	–0.8
	1b	258.2	21.64	–9.5	–1.3
	2a	273.5	17.54	–6.4	–3.9
N ₂	1a	292.1	–	–4.8	–0.4
	1b	268.8	17.83	–7.5	–0.6
	2a	290.0	10.82	–3.9	–2.3
CO	1a	285.0	–	–5.2	–0.5
	1b	261.1	21.09	–8.2	–0.6
	2a	280.4	13.20	–4.4	–2.7
CS	1a	276.3	–	–6.9	–0.7
	1b	253.3	28.03	–10.6	–0.9
	2a	272.8	16.29	–5.8	–3.7
CNH	1a	287.9	–	–4.8	–0.1
	1b	262.6	20.65	–7.6	–0.2
CNLi ^[b]	2a	280.4	13.09	–4.4	–2.2
	1a	301.3	–	–1.2	3.5
	1b	270.0	5.66±4.62	–3.8	4.0
2a	295.3	5.24	–0.2	2.0	

[a] Distances *r*(Cu–Cu) in picometers, force constants *k*(Cu–Cu) in newtons per metre; the attraction energies of the dimers compared to two monomers are given with (ΔE_{CP}) and without (ΔE) CP correction at *r*(Cu–Cu) according to Equations (1) and (2). [b] See ref. [45].

Most striking are the calculated Cu–Cu equilibrium distances r_{eq} (Cu–Cu) (Table 5). First, they show a strong dependency on the nature of the ligand X. Second, they are highly sensitive to the basis set applied. While for X = OH₂ a large equilibrium distance of r_{eq} (Cu–Cu) = 313.9 pm is found (basis 2a), we calculated a much shorter distance for X = CS (r_{eq} (Cu–Cu) = 272.8 pm, Δr_{eq} = 41.1 pm). Such a large ligand effect is not easy to understand. The data suggest that ligands with good σ -donor and π -acceptor capabilities such as X = CS or X = CO result in shorter Cu–Cu bond lengths. It is possible that the π -acceptor ligands are able to withdraw electron density from the formally positively charged copper(II) centers (Cu⁺), so that the Pauli repulsion is decreased and the monomeric fragments move closer together. An NBO analysis supports this (Table 4). Here the CS ligand is more negatively charged, and the Cu 3d orbital population is smaller relative to, for example, the CO ligand due to Cu(*d_π*) → CS(*p_π*) back donation.

As all the interaction potentials at the equilibrium distances are very shallow (see Figure 6), large changes in the Cu–Cu bond lengths do not necessarily cause the interaction energies to change dramatically. As an example, for X = NH₃ the energy change between *r*(Cu–Cu) = 275 pm and *r*(Cu–Cu) = 350 pm (Δr = 75 pm) amounts to only 0.5 kcal mol^{–1}.

Our calculations also reveal that the Cu–Cu distances are a sensitive probe for slight (electronic) changes caused by different basis sets (Table 5). For calculations with basis 1a, relatively long Cu–Cu equilibrium distances are obtained. Reoptimizing the Cu–Cu bond lengths by using two addi-

tional f functions (basis 1b)^[10] causes all Cu–Cu equilibrium distances to decrease by more than 22 pm; for example, for X = OH, Δr (Cu–Cu) = 31.3 pm is calculated. Applying the large basis 2a causes the Cu–Cu bond lengths to decrease by between 1.2 pm (X = SH₂) and 7.5 pm (X = CNH) compared to basis 1a, and to increase by 15.1 pm (X = PH₃) to 26.7 pm (X = OH₂) compared to basis 1b.

The variations in the Cu–Cu bond lengths due to the different quality of the basis sets are also reflected in the attraction energies between the monomers. When we originally started these calculations with basis set 1a, we realized that the counterpoise (CP) correction for the BSSE to the monomer energies almost completely cancelled the attraction between the monomers in the supermolecule (compare ΔE and ΔE_{CP} at the *r*(Cu–Cu) distances of the CP-uncorrected dimer in Table 5 and Figure 7). Furthermore, in some cases

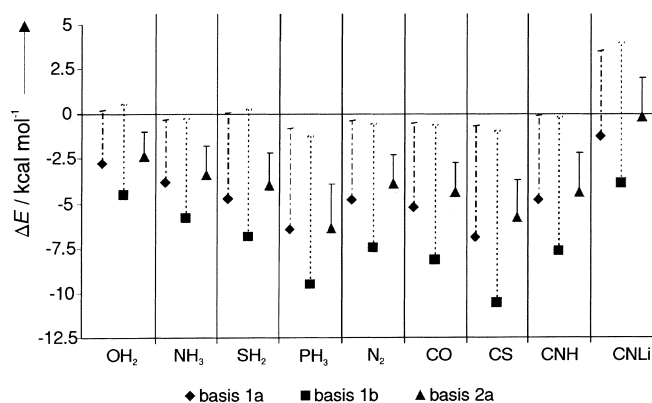


Figure 7. Attraction energies ΔE for the dimers **7**. The error bars show the BSSE and the resulting ΔE_{CP} values at the corresponding equilibrium distances r_{eq} (Cu–Cu).

(e.g., X = OH₂, SH₂, CNLi) we obtained purely repulsive potential curves. According to Equations (1) and (2) the $\Delta_{CP}\Delta E$ values (difference between ΔE and ΔE_{CP}) are between $\Delta_{CP}\Delta E$ = 3.0 kcal mol^{–1} (X = OH₂) and $\Delta_{CP}\Delta E$ = 6.2 kcal mol^{–1} (X = CS), which is of the order of the actual attraction energy; this is exactly the problem others faced.^[10, 13, 21] In fact, the BSSE increases from basis set 1a to the larger basis set 1b and is then in the range of $\Delta_{CP}\Delta E$ = 5.1 kcal mol^{–1} (X = OH₂) and $\Delta_{CP}\Delta E$ = 9.6 kcal mol^{–1} (X = CS). This suggests that the basis set is less than complete in the spd part, or important higher angular momentum functions are missing.

To analyze the BSSE in more detail we studied different basis sets for different atoms. The BSSE increases on adding two f functions to Cu, and this suggests that the basis set at the copper center is mainly responsible for this error, as one would expect. In fact calculations for X = CO indicate that the BSSE decreases by only 3% if the basis set 1b on the heteroatoms is extended from 6-31 + G(d) to the Dunning cc-pVTZ basis.^[36] On the other hand, if the monomer is calculated by taking only the Gaussian basis functions at the center of the second (ghost) copper atom (see Figure 8, structure **D**) into account about 70% of the BSSE is recovered (between 55 and 60% for basis 1a).

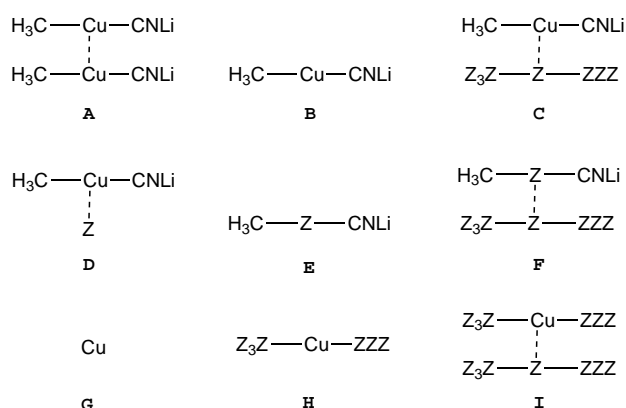


Figure 8. Schematic structures of calculated molecules to study the BSSE. Z denotes the atoms which were treated as “ghost” atoms, that is, the Gaussian basis functions at the corresponding atom position where taken into account.

We therefore decided to optimize the copper basis set at the correlated (MP2) level to suppress errors in the spdf part before adding higher angular momentum functions,^[46] as described in the computational section. This technique eliminated most of the BSSE for the notoriously difficult molecule Hg_2 .^[47] Our systematic investigation on the BSSE using this newly developed basis for copper (see Table 2) is summarized in Table 6.

Table 6. The basis set superposition error for CH_3CuCNLi .^[a]

Structure	Basis set ^[b]	E	ΔE
A	6-31 + G(d)/Cu _{UCC}	− 674.15472	–
B	6-31 + G(d)/Cu _{UCC}	− 337.07678	–
C	6-31 + G(d)/Cu _{UCC}	− 337.08016	− 2.12
D	6-31 + G(d)/Cu _{UCC}	− 337.07865	− 1.17
E	6-31 + G(d)/Cu _{UCC}	− 139.74643	–
F	6-31 + G(d)/Cu _{UCC}	− 139.74885	− 1.52
G	6-31 + G(d)/Cu _{UCC}	− 197.13703	–
H	6-31 + G(d)/Cu _{UCC}	− 197.13914	− 1.32
I	6-31 + G(d)/Cu _{UCC}	− 197.13847	− 0.90
A	cc-pVTZ/Cu _{UCC}	− 674.52230	–
B	cc-pVTZ/Cu _{UCC}	− 337.26113	–
C	cc-pVTZ/Cu _{UCC}	− 337.26299	− 1.16

[a] The structure fragments **A–I** are shown in Figure 8. The total electronic energies E for **A–I** are given in au, and the relative energies ΔE in kcal mol^{-1} . [b] All heteroatoms were calculated by using either the 6-31 + G(d) or cc-pVTZ basis sets.^[36] Cu_{UCC} denotes that for copper the uncontracted correlation-consistent basis set (see Table 2) was used.

The BSSE per monomer ($X = \text{CNLi}$) now drops from $\Delta_{\text{CP}}\Delta E = 3.9 \text{ kcal mol}^{-1}$ (basis 1b) to $\Delta_{\text{CP}}\Delta E = 2.2 \text{ kcal mol}^{-1}$ (−44%) for the 6-31 + G(d) basis sets by applying the Cu correlation-consistent basis set together with the heteroatoms. To reduce the remaining error even further, a more detailed study of the single fragments was necessary. For example, comparison of structure **D** with **C** (Figure 8) reveals that $1.2 \text{ kcal mol}^{-1}$ (55%) of the remaining $2.2 \text{ kcal mol}^{-1}$ originated from the second copper atom only. However, comparing structures **F** and **E** reveals that the ligand atoms are responsible for $1.5 \text{ kcal mol}^{-1}$ (70%) of the BSSE. This leads to the conclusion that the BSSE arising from the ligand atoms is now of the same magnitude as that resulting from the

copper atom. Furthermore if the ligand basis is extended from 6-31 + G(d) to cc-pVTZ (Table 6) the BSSE again drops by nearly 50% (cf. **B** and **C**) to a final value of $1.2 \text{ kcal mol}^{-1}$ per monomer fragment. In fact, from the error bars given for the different ligands **X** in Figure 7 it is clear that basis 2a reduces the BSSE in general by approximately 70% relative to basis 1b, while the error compared to basis 2a is reduced by at least 50% for basis 1a.

Finally, for $X = \text{NH}_3$ and $X = \text{PH}_3$, CP-corrected potential curves (for $X = \text{PH}_3$, see Figure 9) were calculated with basis 1b and basis 2a to study the BSSE for the entire range between $r(\text{Cu–Cu}) = 200$ and 400 pm .

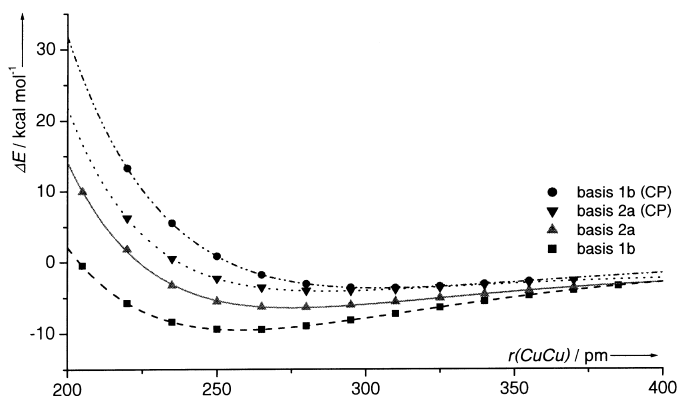


Figure 9. Potential energy curves of $[(\text{CH}_3\text{CuPH}_3)_2]$ calculated by using basis sets 1b and 2a with and without counterpoise (CP) correction. The $\Delta E [\text{kcal mol}^{-1}]$ values are given relative to the energy of the two monomers.

For basis 2a and $X = \text{PH}_3$, the BSSE increases the Cu–Cu equilibrium distance from $r_{\text{eq}}(\text{Cu–Cu}) = 273.5$ to $r_{\text{eq}}(\text{CuCu}) = 289.1 \text{ pm}$ ($\Delta r(\text{Cu–Cu}) = 15.6 \text{ pm}$) and the cuprophilic attraction from $\Delta E_{\text{CP}} = -3.9$ to $-4.1 \text{ kcal mol}^{-1}$ compared to the CP-corrected values at the original bond length. In the case of $X = \text{NH}_3$, $r(\text{Cu–Cu})$ changes from 304.3 to 326.3 pm ($\Delta r(\text{Cu–Cu}) = 22.0 \text{ pm}$) and ΔE_{CP} from -1.8 to $-2.0 \text{ kcal mol}^{-1}$. To summarize, correlation-consistent basis sets for the copper atom and the ligands (e.g., basis 2a) remove most of the BSSE and should therefore be preferred over standard HF-optimized sets for weak metal–metal interactions.

Various empirical relationships between metal–metal distances and force constants have been developed in the past.^[48] The Hershbach–Laurie rule^[49] has been used successfully to describe dinuclear transition metal complexes (e.g., $M = \text{Cr}, \text{Mo}, \text{Rh}, \text{Pd}, \text{Ag}, \text{W}, \text{Re}, \text{Ir}, \text{Pt}, \text{Au}, \text{Hg}$), as reviewed by Harvey.^[48] We therefore applied the Hershbach–Laurie equation [Eq. (4)] to fit the optimized equilibrium distance $r_{\text{eq}}(\text{Cu–Cu}) [\text{pm}]$ of the dimers **7** to the logarithm of the calculated force constant $k(\text{Cu–Cu}) [\text{N m}^{-1}]$ obtained from a Morse fit, as shown in Table 5.

$$r(\text{Cu–Cu}) = a + b(\ln k/100) \quad (4)$$

The results for basis sets 1b and 2a (from Table 5) are plotted in Figure 10. Linear regression yields for basis 1b (basis 2a) values of $a = 227.8$ ($a = 227.6$) and $b = -23.0$ ($b =$

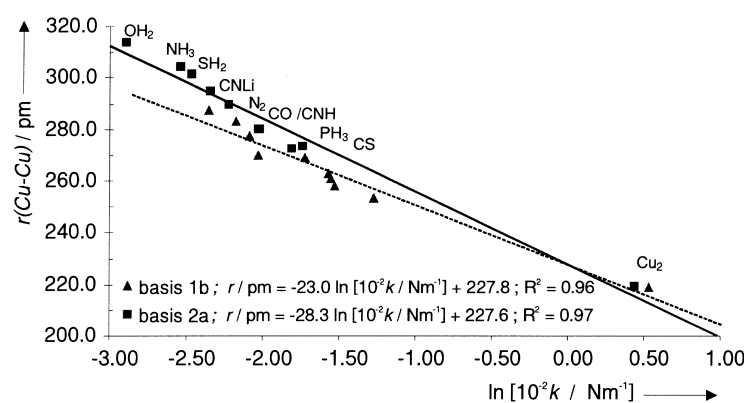


Figure 10. Hershbach–Laurie fit for all calculated dimers $(\text{CH}_3\text{CuX})_2$ and Cu_2 according to Table 5 and Equation (4).

–28.3), which essentially differ only in the slope. Interestingly, the b values are of the same magnitude as the published values for Ag and Au (Table 7), and only the intercept increases on going from Cu to Au.

Table 7. Hershbach–Laurie parameters for Group 11 elements according to Equation (4).

M	a [pm]	b [pm]	Ref.
Cu	228	–22.8	this work ^[a]
	228	–28.3	this work ^[b]
Ag	250	–30.0	[4]
	253	–28.4	[48]
Au	268	–29.0	[4]
	289	–20.6	[53]
	325	–29.0	[2b]

[a] Calculated with basis 1b. [b] Calculated with basis 2a.

To the best of our knowledge, no experimental parameters a and b are available for the Cu_2 system. Hence, given the Cu–Cu bond length, our formula allows the first crude estimates of Cu–Cu stretching force constants $k(\text{Cu–Cu})$, or vice versa, to be made; this is important for future vibrational studies in solution or the solid state. For example, taking the experimental $\text{Cu}^{\text{I}}\text{–Cu}^{\text{I}}$ stretching frequency ($\tilde{\nu}(\text{Cu}_2) = 104 \text{ cm}^{-1}$) of $[\text{Cu}_2(\text{dcpm})_2]\text{X}_2$,^[34] we obtain the force constant $k(\text{Cu–Cu})$ within the harmonic approximation. Substituting the calculated value of $k(\text{Cu–Cu}) = 20.05 \text{ Nm}^{-1}$ into the Hershbach–Laurie formula [Eq. (4)], together with the given a and b values (basis 2a), we obtain a bond length of $r(\text{Cu–Cu}) = 273.1 \text{ pm}$, in perfect agreement with the experimentally determined value of $r(\text{Cu–Cu}) = 273.1 \text{ pm}$.

Relativistic effects on the Cu–Cu bond lengths and interactions were calculated to be rather small, at least for $\text{X} = \text{NH}_3$. A slightly longer Cu–Cu bond length of 305.5 pm and a essentially unchanged attraction of $\Delta E = 3.41 \text{ kcal mol}^{-1}$ were found in the nonrelativistic case, as compared to 304.3 pm and $\Delta E = 3.43 \text{ kcal mol}^{-1}$ in the relativistic case.

We also studied the influence of bent monomer units **6** on the Cu–Cu interaction in the dimers **7** (see Table 8). Dimers with slightly bent monomer units ($\alpha(\text{C–Cu–X}) < 180^\circ$) are more favourable than those with linear monomers ($\alpha(\text{C–Cu–X}) = 180^\circ$). For $\text{X} = \text{NH}_3$ (CS) we calculated an optimum monomer angle of $\alpha(\text{C–Cu–X}) = 178.8^\circ$ (175.3°). Most striking

is that the Cu–Cu bond of the dimer is significantly shorter if the monomers are bent, in agreement with the findings of Liu et al.^[13] For example, for $\text{X} = \text{CS}$ with $\alpha(\text{C–Cu–X}) = 175.0^\circ$ we calculate an equilibrium distance of $r(\text{Cu–Cu}) = 264.8 \text{ pm}$ (Table 8), which is 8 pm shorter than the equilibrium distance of $r(\text{Cu–Cu}) = 272.8 \text{ pm}$ for $\alpha(\text{C–Cu–X}) = 180^\circ$. A similar result was found for $\text{X} = \text{NH}_3$. The calculated effect on the attraction of two monomers [Eq. (1)] is relatively

small ($< 0.5 \text{ kcal mol}^{-1}$) but not negligible. This suggests that the copper–copper interactions, which increase on bending the monomers, are responsible for the bent monomers in crystals of compound such as **5** ($\alpha(\text{C–Cu–C}) = 172.9$ and 171.3°), although the bending is often discussed only as consequence of lithium coordination. Note that the $t\text{Bu–Cu}(\text{CN})\text{Li}$ monomers in **4** are also bent ($\alpha(\text{C–Cu–C}) = 170.0$ and 168.0°), although **4** contains no bridging lithium atoms.

Table 8. The Cu–Cu attraction as a function of the angle $\alpha(\text{C–Cu–X})$ [$^\circ$]. The $r(\text{Cu–Cu})$ [pm] and ΔE [kcal mol^{-1}] values are optimized for the corresponding angle α .^[a]

α	$\text{X} = \text{NH}_3$		$\text{X} = \text{CS}$	
	$r(\text{Cu–Cu})$	ΔE	$r(\text{Cu–Cu})$	ΔE
180	304.3	–3.43	272.8	–5.83
175	292.9	–3.21	264.8	–6.16
170	283.0	–2.17	259.2	–5.74
165	275.9	–0.32	255.1	–4.53

[a] A polynomial fit of the angle α to the interaction energy ΔE yields for $\text{X} = \text{NH}_3$ (CS) an optimal angle of $\alpha(\text{C–Cu–X}) = 178.8^\circ$ (175.3°), which corresponds to a Cu–Cu bond length of $r(\text{Cu–Cu}) = 301.5$ (265.1 pm).

Tetramer: To study whether the inward bending in compounds like **1–3** is due to ring constraints or to cuprophilic interactions we optimized the model compound $(\text{CH}_3\text{Cu})_4$ (**8**) at the HF and MP2 levels of theory (Figure 11). At both levels of theory an inward-bent C–Cu–C arrangement is found. Since we showed in the previous section that HF only produces repulsive energy curves, we conclude that the bending also occurs if cuprophilic interactions are absent. The question then is to what extent cuprophilic interactions influence the structure of such compounds.

To obtain some indication of cuprophilic interactions in this tetrameric copper compound we performed the following steps:

- 1) Starting with the HF-optimized structure we switched on correlation effects (at the MP2 level) to see whether cuprophilic interactions decrease the C–Cu–C bond angles and Cu–Cu bond lengths. Since the C–Cu bond at the MP2 level is shorter than that at the HF level of theory, this contraction in the C–Cu bond due to correlation effects will counteract the cuprophilic interaction.

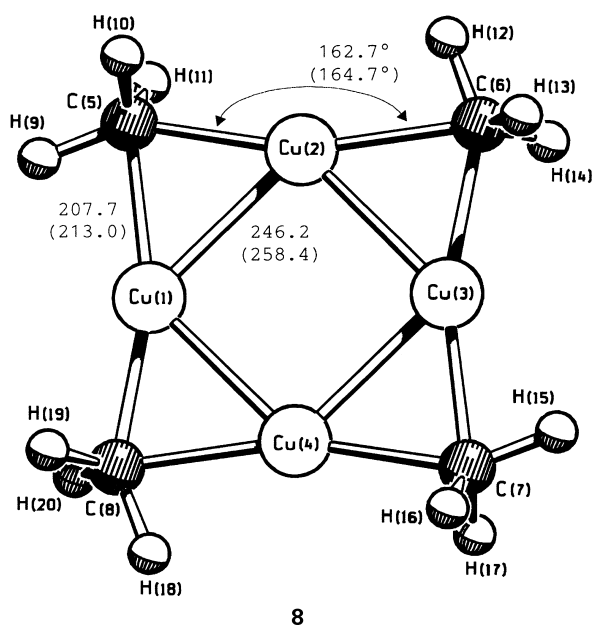


Figure 11. Optimized MP2 structure of **8**. HF values are given in parentheses.

2) Starting with the MP2-optimized structure we switched correlation effects off (HF level) to see if the absence of cuprophilic interactions increases the C–Cu–C bond angles and the Cu–Cu bond lengths. Since the C–Cu bond at the HF level is longer than that at the MP2 level of theory, this contribution will counteract the increase in the C–Cu–C bond angle.

For case 1 the Cu–Cu bond length decreases by 8.0 pm, and the C–Cu–C bond angle decreases by 3.0°. The stabilization energy for this process is 1.3 kcal mol⁻¹. For case 2 the Cu–Cu bond length increases by 6.6 pm, and the C–Cu–C angle by 2.6°. The energy gain for this process is 4.4 kcal mol⁻¹. Although LANL2DZ basis sets and pseudopotentials may overestimate cuprophilic interactions, these changes clearly indicate that cuprophilic interactions are partly responsible for the short Cu–Cu bonds and C–Cu–C bending in structures such as **1–3**.

Conclusion

We have clearly established the existence of cuprophilic interactions for a number of different compounds. By successively eliminating the BSSE by applying correlation-consistent valence basis sets together with a small core pseudopotential for copper, the CSIs were found to be attractive by up to 4 kcal mol⁻¹ for a number of model compounds. Cuprophilic interactions are therefore approximately three times weaker than aurophilic interactions. Although we modelled these interactions for compounds known in the solid state, some of these cuprophilic interactions may be large enough to exist in dimeric cuprates in solution, as suggested by Boche et al.^[32]

Acknowledgements

This work was supported by the Alexander von Humboldt Foundation (Bonn, Germany), SFB260 (Deutsche Forschungsgemeinschaft, Germany), the Graduierten-Kolleg Metallorganische Chemie, Philipps-Universität Marburg (Deutsche Forschungsgemeinschaft, Germany), the Marsden Fund (Wellington, New Zealand), and the Auckland University Research Committee.

- [1] M. Jansen, *Angew. Chem.* **1987**, *99*, 1136; *Angew. Chem. Int. Ed. Engl.* **1987**, *26*, 1043.
- [2] a) J. B. Foley, A. E. Bruce, M. R. M. Bruce, *J. Am. Chem. Soc.* **1995**, *117*, 9596; b) P. Schwerdtfeger, A. E. Bruce, M. R. M. Bruce, *J. Am. Chem. Soc.* **1998**, *120*, 6587; c) C. King, J.-C. Wang, M. N. I. Khan, J. P. Fackler, Jr., *Inorg. Chem.* **1989**, *28*, 2145; d) E. J. Fernández, M. C. Gimeno, A. Laguna, J. M. López-de-Luzuriaga, M. Monge, P. Pykkö, D. Sundholm, *J. Am. Chem. Soc.* **2000**, *122*, 7287.
- [3] R. Hoffmann, *Angew. Chem.* **1982**, *94*, 725; *Angew. Chem. Int. Ed. Engl.* **1982**, *21*, 711.
- [4] D. Perreault, M. Drouin, V. M. Minkowski, W. P. Schaefer, P. D. Harvey, *Inorg. Chem.* **1992**, *31*, 695.
- [5] B. Krebs, *Unkonventionelle Wechselwirkungen in der Chemie der metallischen Elemente*, VCH, Weinheim, **1992**.
- [6] R. Wesendrup, P. Schwerdtfeger, *Angew. Chem.* **2000**, *112*, 938; *Angew. Chem. Int. Ed.* **2000**, *39*, 907.
- [7] P. Pykkö, *Chem. Rev.* **1997**, *97*, 597.
- [8] H. Schmidbaur, *Chem. Soc. Rev.* **1995**, 394.
- [9] a) P. Pykkö, N. Runeberg, F. Mendizabal, *Chem. Eur. J.* **1997**, *3*, 1458; b) P. Pykkö, F. Mendizabal, *Inorg. Chem.* **1998**, *37*, 3018; c) P. Pykkö, T. Tamm, *Organometallics*, **1998**, *17*, 4842.
- [10] P. Pykkö, N. Runeberg, F. Mendizabal, *Chem. Eur. J.* **1997**, *3*, 1451.
- [11] N. Runeberg, M. Schütz, H.-J. Werner, *J. Chem. Phys.* **1999**, *110*, 7210.
- [12] a) C. King, J. C. Wang, S. Wang, M. N. I. Khan, J. P. Fackler, Jr., *Inorg. Chem.* **1988**, *27*, 1672; b) C.-M. Che, H. L. Kwong, V. W. Yam, C. K. Cho, *J. Chem. Soc. Chem. Commun.* **1989**, 855; c) L. H. Gam, *Angew. Chem.* **1997**, *109*, 1219; *Angew. Chem. Int. Ed. Engl.* **1997**, *36*, 1171; d) D. L. Phillips, K. H. Leung, M.-C. Tse, C.-M. Che, V. M. Miskowski, *J. Am. Chem. Soc.* **1999**, *121*, 4799.
- [13] X.-Y. Liu, F. Mota, P. Alemany, J. J. Novoa, S. Alvarez, *Chem. Commun.* **1998**, 1149.
- [14] R. Ahlrichs, C. Kölmel, *J. Phys. Chem.* **1990**, *94*, 5536.
- [15] a) C. He, J. L. DuBois, B. Hedmann, K. O. Hedgson, S. J. Lippard, *Angew. Chem.* **2001**, *113*, 1532; *Angew. Chem. Int. Ed.* **2001**, *40*, 1484; b) I. Dance, C. Horn, D. Craig, M. Scudder, G. Bowmaker, *J. Am. Chem. Soc.* **1998**, *120*, 10549.
- [16] a) U. Siemeling, U. Vorfeld, B. Neumann, H.-G. Stämmler, *Chem. Commun.* **1997**, 1723; b) P. Stavropoulos, K. Singh, J. R. Long, *J. Am. Chem. Soc.* **1997**, *119*, 2942.
- [17] a) K. Mehrotra, R. Hoffmann, *Inorg. Chem.* **1978**, *17*, 2187; b) R. Hoffmann, A. Dedieu, *J. Am. Chem. Soc.* **1978**, *100*, 2074; c) Y. Jiang, S. Alvarez, R. Hoffmann, *Inorg. Chem.* **1985**, *24*, 749.
- [18] F. J. Hollander, D. Coucouvanis, *J. Am. Chem. Soc.* **1974**, *96*, 5646.
- [19] a) A. Avdeef, J. P. Fackler, Jr., *Inorg. Chem.* **1978**, *17*, 2182; b) J.-M. Poblet, M. Bénard, *Chem. Commun.* **1998**, 1179.
- [20] a) F. A. Cotton, M. Matusz, R. Poli, X. Feng, *J. Am. Chem. Soc.* **1988**, *110*, 7077; b) F. A. Cotton, X. Feng, D. J. Timmons, *Inorg. Chem.* **1998**, *37*, 4066.
- [21] E. Ruiz, S. Alvarez, P. Alemany, R. A. Evarestov, *Phys. Rev. B* **1997**, *56*, 7189.
- [22] H. Schumann, C. Janiak, J. Pickardt, U. Börner, *Angew. Chem.* **1987**, *99*, 788; *Angew. Chem. Int. Ed. Engl.* **1987**, *26*, 789.
- [23] a) C. Janiak, R. Hoffmann, *Angew. Chem.* **1989**, *101*, 1706; *Angew. Chem. Int. Ed. Engl.* **1989**, *28*, 1688; b) C. Janiak, R. Hoffmann, *J. Am. Chem. Soc.* **1990**, *112*, 5924.
- [24] P. Schwerdtfeger, *Inorg. Chem.* **1991**, *30*, 1660.
- [25] The shortest determined Cu–Cu bond length ($r(\text{Cu}–\text{Cu}) = 235$ pm) was found for tris[1,5-ditolylpentaazadienidocopper(II)], which is far shorter than that in the metal ($r(\text{Cu}–\text{Cu}) = 256$ pm): J. Strähle, J. Beck, *Angew. Chem.* **1985**, *97*, 419; *Angew. Chem. Int. Ed. Engl.* **1985**, *24*, 409; long bonds are found in compounds such as $[\text{Ph}_3\text{PCuBr}]_4$ with

- $r(\text{Cu}-\text{Cu}) = 345 \text{ pm}$: M. R. Churchill, K. L. Kalra, *J. Am. Chem. Soc.* **1973**, *95*, 5772.
- [26] a) G. van Koten, S. L. James, J. T. B. H. Jastrzebski in *Comprehensive Organometallic Chemistry II, Vol. 3* (Eds.: E. W. Abel, F. G. A. Stone, G. Wilkinson), Pergamon/Elsevier, Oxford, **1995**, p. 57; b) B. J. Hathaway in *Comprehensive Coordination Chemistry, Vol. 5* (Ed.: G. Wilkinson), Pergamon/Elsevier, Oxford, **1987**, p. 533.
- [27] J. A. J. Jarvis, M. F. Lappert, B. T. Kilbourn, R. Pearce, *J. Chem. Soc. Chem. Commun.* **1973**, 475.
- [28] D. Nobel, G. van Koten, A. L. Spek, *Angew. Chem.* **1989**, *101*, 211; *Angew. Chem. Int. Ed. Engl.* **1989**, *28*, 208.
- [29] G. van Koten, J. G. Noltes in *Fundamental Research in Homogeneous Catalysis, Vol. 3* (Eds.: M. Tsutsui, R. Ugo), Plenum, New York, **1979**, p. 953.
- [30] a) J. M. Zuo, M. Kim, M. O'Keeffe, J. C. H. Spence, *Nature* **1999**, *421*, 49; b) W. H. E. Schwarz, S.-G. Wang, *Angew. Chem.* **2000**, *112*, 1827; *Angew. Chem. Int. Ed.* **2000**, *39*, 1757; c) J. M. Zuo, M. Kim, M. O'Keeffe, J. C. H. Spence, *Angew. Chem.* **2000**, *112*, 3947; *Angew. Chem. Int. Ed.* **2000**, *39*, 3791; d) W. H. E. Schwarz, S.-G. Wang, *Angew. Chem.* **2000**, *112*, 3950; *Angew. Chem. Int. Ed.* **2000**, *39*, 3794.
- [31] G. Boche, F. Bosold, M. Marsch, K. Harms, *Angew. Chem.* **1998**, *110*, 1779; *Angew. Chem. Int. Ed.* **1998**, *37*, 1684.
- [32] M. John, C. Auel, C. Behrens, M. Marsch, K. Harms, F. Bosold, R. M. Geschwind, P. R. Rajamohanan, G. Boche, *Chem. Eur. J.* **2000**, *6*, 3060.
- [33] From solvents that solvate Li^+ well or from ligands (THF, [12]crown-4, amines, etc.), lithium cuprates $\text{R}_2\text{CuLi}(\cdot\text{LiX})$ crystallize as a solvent-separated ion pairs (SSIP) with almost linear C-Cu-C angles; see ref. [32].
- [34] C.-M. Che, Z. Mao, V. M. Miskowski, M.-C. Tse, C.-K. Chan, K.-K. Cheung, D. L. Phillips, K.-H. Leung, *Angew. Chem.* **2000**, *112*, 4250; *Angew. Chem. Int. Ed.* **2000**, *39*, 4084.
- [35] M. J. Frisch, G. W. Trucks, H. B. Schlegel, G. E. Scuseria, M. A. Robb, J. R. Cheeseman, V. G. Zakrzewski, J. A. Montgomery, Jr., R. E. Stratmann, J. C. Burant, S. Dapprich, J. M. Millam, A. D. Daniels, K. N. Kudin, M. C. Strain, O. Farkas, J. Tomasi, V. Barone, M. Cossi, R. Cammi, B. Mennucci, C. Pomelli, C. Adamo, S. Clifford, J. Ochterski, G. A. Petersson, P. Y. Ayala, Q. Cui, K. Morokuma, D. K. Malick, A. D. Rabuck, K. Raghavachari, J. B. Foresman, J. Cioslowski, J. V. Ortiz, B. B. Stefanov, G. Liu, A. Liashenko, P. Piskorz, I. Komaromi, R. Gomperts, R. L. Martin, D. J. Fox, T. Keith, M. A. Al-Laham, C. Y. Peng, A. Nanayakkara, C. Gonzalez, M. Challacombe, P. M. W. Gill, B. G. Johnson, W. Chen, M. W. Wong, J. L. Andres, M. Head-Gordon, E. S. Replogle, J. A. Pople, Gaussian98, Revision A.1, Gaussian, Pittsburgh PA, **1998**.
- [36] The 6-31 + G(d) basis set and the correlation-consistent basis sets of Dunning et al. were used as implemented in Gaussian98; see ref. [35].
- [37] M. Dolg, U. Wedig, H. Stoll, H. Preuss, *J. Chem. Phys.* **1987**, *86*, 866.
- [38] a) C. E. Moore, *Atomic Energy Levels*, U.S. GPO, Washington, **1958**; b) H. Hotop, W. C. Lineberger, *J. Phys. Chem. Ref. Data* **1985**, *14*, 731.
- [39] a) R. Wesendrup, L. Kloo, P. Schwerdtfeger, *Int. J. Mass. Spectrom.* **2000**, *201*, 17; b) J. M. Martin, A. Sundermann, *J. Chem. Phys.* **2001**, *114*, 3408.
- [40] S. F. Boys, F. Bernadi, *Mol. Phys.* **1985**, *19*, 553.
- [41] All electrons were included in the correlation treatment.
- [42] a) J. P. Foster, F. Weinhold, *J. Am. Chem. Soc.* **1980**, *102*, 7211; b) A. E. Reed, F. Weinhold, *J. Chem. Phys.* **1983**, *78*, 4066; c) A. E. Reed, R. B. Weinstock, F. Weinhold, *J. Chem. Phys.* **1985**, *83*, 735; d) A. E. Reed, F. Weinhold, *J. Chem. Phys.* **1985**, *83*, 1736; e) J. E. Carpenter, F. Weinhold, *J. Mol. Struct.: THEOCHEM* **1988**, *169*, 41; f) A. E. Reed, L. A. Curtiss, F. Weinhold, *Chem. Rev.* **1988**, *88*, 899.
- [43] a) C. W. Bauschlicher, S. R. Langhoff, H. Partridge, L. A. Barnes, *J. Chem. Phys.* **1989**, *91*, 2399; b) L. A. Barnes, M. Rosi, C. W. Bauschlicher, *J. Chem. Phys.* **1990**, *93*, 609.
- [44] I. Antes, G. Frenking, *Organometallics* **1995**, *14*, 4263.
- [45] For X = CNLi we obtained a potential energy curve with a repulsive barrier; this compound is metastable with the minimum approximately 1 kcal mol⁻¹ above the dissociation limit.
- [46] A single g function was tested but gave no further improvement at least for the calculated electron affinity E_A and the ionization potential (IP).
- [47] P. Schwerdtfeger, R. Wesendrup, G. E. Moyano, A. Sadlej, J. N. Greif, F. Hensel, *J. Chem. Phys.*, in press.
- [48] Details of the different relations and equations are given in P. H. Harvey, *Coord. Chem. Rev.* **1996**, *153*, 175.
- [49] D. R. Hershbach, V. W. Laurie, *J. Chem. Phys.* **1961**, *35*, 458.
- [50] For the ligands X we calculated with basis 1a/1b (basis 2a) the following bond lengths ($r(\text{X}-\text{Y})$ [pm]): X = OH₂ 97.1 (96.6), X = NH₃ 101.7 (101.7), X = SH₂ 134.0 (134.3), X = PH₃ 141.4 (141.9), X = N₂ 113.1 (111.0), X = CO 115.1 (113.5), X = CS 154.2 (153.9), X = CNH $r(\text{C}-\text{N})$ 117.8 (117.5) $r(\text{N}-\text{H})$ 107.1 (100.6), X = CNLi $r(\text{C}-\text{N})$ 119.2 (118.6) $r(\text{N}-\text{Li})$ 191.8 (181.5).
- [51] a) M. Böhme, G. Frenking, *Chem. Phys. Lett.* **1994**, *224*, 195; b) M. Böhme, G. Frenking, M. T. Reetz, *Organometallics* **1994**, *13*, 4237.
- [52] a) E. Nakamura, S. Mori, M. Nakamura, K. Morokuma, *J. Am. Chem. Soc.* **1997**, *119*, 4887; b) E. Nakamura, S. Mori, K. Morokuma, *J. Am. Chem. Soc.* **1997**, *119*, 4900; c) E. Nakamura, M. Nakamura, Y. Miyachi, N. Koga, K. Morokuma, *J. Am. Chem. Soc.* **1993**, *115*, 99.
- [53] Ab initio value for (X₂AuPH₃)₂ model systems: P. Pyykkö, J. Li, N. Runeberg, *Chem. Phys. Lett.* **1994**, *218*, 133.

Received: May 9, 2001 [F3248]